JETIR.ORG ISSN: 2349-5162 | ESTD Year : 2014 | Monthly Issue

JOURNAL OF EMERGING TECHNOLOGIES AND INNOVATIVE RESEARCH (JETIR)

An International Scholarly Open Access, Peer-reviewed, Refereed Journal

Design and Implementation of FOC and GUI for EV Test Bench in LabVIEW

[1]Pradeep Kumar S, [2]Dr. Dinesh M N

[1]PG Student, [2]Professor

[1]Department of Electrical and Electronics,

[1]RV College of Engineering, Bengaluru, India

Abstract : The rising popularity and demand for electric vehicles have been increasing rapidly in recent years. The EV motor before being installed in the vehicle is to be analyzed and calibrated by emulating the real-time load conditions in a dyno test bench. The EV motor being tested – Device Under Test (DUT) is required to operate in an error-free control system for the performance analysis. The Field Oriented Control (FOC) algorithm suits the required motor control criteria to operate the motor with direct torque control and field weakening control. The FOC algorithm is developed in LabVIEW using cRIO9046, FPGA modules NI9223(Analog input module – 1MS/s) and NI9401(Digital IO – 10MHz) to process at 47us operating in real-time. The PMSM motor is considered a DUT motor, the control of the DUT motor is achieved in torque mode to test DUT in all 4-quadrant operations of the motor. The GUI developed allows the user to set the speed, and display all waveforms. Speed to the equivalent Iq reference value is obtained through a look-up table and the motor operates in direct torque control (DTC) mode up to the base speed of the motor. The Id reference control using the lookup table provides speed control up to the peak speed of the motor with reduced torque on on-load conditions. The DUT motor tested is an 8-pole PMSM motor with peak power of 60kW and peak speed of 4000rpm. The FOC control system in LabVIEW offers robust control of the motor by operating the motor in all 4 quadrant operations, the motor achieves the set speed from standstill in 3 seconds on the no-load condition and achieves the set speed in 6 seconds on the on-load condition at 1000rpm, 10Nm.

IndexTerms **- LabVIEW, Field Oriented Control, Permanent Magnet Synchronous Motor, Device Under Test.**

I. INTRODUCTION

EV motors need to be analyzed and calibrated before being installed in a vehicle by emulating the real-time load conditions in a dyne test bench. The loading capacity of the vehicle, maximum driving speed, acceleration, deceleration rate, maximum power, torque on wheels etc. can be analyzed based on the load driving capacity of the motor. The EV motor being tested – Device Under Test (DUT) is required to operate in an error-free control system for the performance analysis. Compared to the six-step commutation control and hysteresis current control the field- oriented control (FOC) delivers fast acceleration and deceleration of motor giving more accurate and better speed control with less torque ripple and fast torque response. The Field Oriented Control (FOC) algorithm suits the required motor control criteria to operate the motor with direct torque control and field weakening control.

The FOC algorithm is developed in LabVIEW – the real time graphical software tool, to run the DUT motor in all 4 quadrant operations – forward motoring, forward braking, reverse motoring and reverse braking. The reverse re-generative braking with damping load may be considered in EV test bench. The National Instruments' cRIO-9046, real time module is considered for the interface of the FPGA modules NI9223 – analog input module as analog to digital converter (ADC) to read physical feedback signals and NI9401 – digital input-output module to generate pulse width modulation (PWM) signals on processing the FOC algorithm.

The conventional drive system uses the three types of motors that have become popular in electric drive applications- PMSM motor, brushless DC motor and three - phase induction motor [1]. The PMSM motor is considered for user end application and testing – Device Under Test (DUT) as it is more reliable, less noisy, has higher efficiency, delivers high torque and offers better `performance in both low and high-speed operations than other motors.

The FOC algorithm developed in LabVIEW processes each iteration in 47us to operate the DUT motor in real-time with less torque ripple and fast torque response. The DUT motor is mounted on a 350kW dyne test-bench and operated in torque mode to drive the DUT -PMSM motor at various load conditions up to rated speed of 2500rpm with load torque of 22Nm.

II. EV DYNE TEST BENCH AND FIELD ORIENTED CONTROL

2.1 EV DYNE TEST BENCH

The EV dyne motor test bench is a platform which evaluates the measure of torque and rotational speed, giving a reading that indicates the power of the motor. In dyne load test the DUT motor is initially operated at the no-load condition at its peak power assuring safe operating conditions. The DUT motor is now loaded lightly by the dyne motor, gradually loading the DUT motor to its full load operating capacity. The dyne motor is operating below the rated speed of DUT motor to avoid stalling

. The speed of the DUT motor is set at a fixed value and the load is applied to a known value and the variation in speed and load torque experienced is recorded. These recorded data is now used to analyse the maximum operable speed, torque and power of the motor. The load conditions equivalent to the load experienced by EV motor in an electric vehicle on road and the 4 quadrant operations – forward motoring, forward braking, reverse motoring and reverse braking of motor loading is tested. The performance and efficiency of the DUT motor is now evaluated and the benchmarking is done for the electric vehicle's maximum rated speed, torque and power.

2.2 FIELD ORIENTED CONTROL

The Field Oriented Control is a vector control method in which the three phase stator currents – I_a, I_b and I_c of the DUT motor are transformed as equivalent two-phase orthogonal components that can be visualized as constant vectors I_d and I_q. The d-q current components are modulated according to the set speed in the PI controllers. The modulated output from the PI controllers is the equivalent voltage components V_d and V_q. These d-q voltage components are transformed to equivalent 3 phase voltages V_a,V_b and V_c. These 3 phase voltage components are compared with high frequency triangle wave of 5kHz to obtain the sinusoidal pulse width modulation (SPWM) signals. The summary of the FOC algorithm is shown in fig.1 – Summary of FOC.

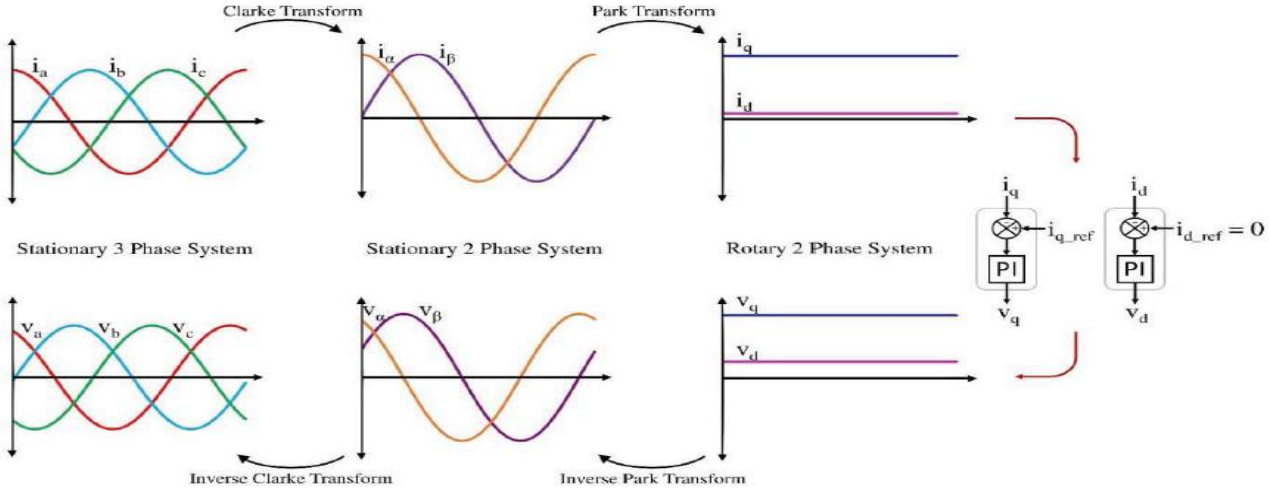

Fig-1: Summary of Field Oriented Control (FOC) algorithm

III. FUNCTIONAL BLOCK DIAGRAM AND METHODOLOGY

3.1 FUNCTIONAL BLOCK DIAGRAM

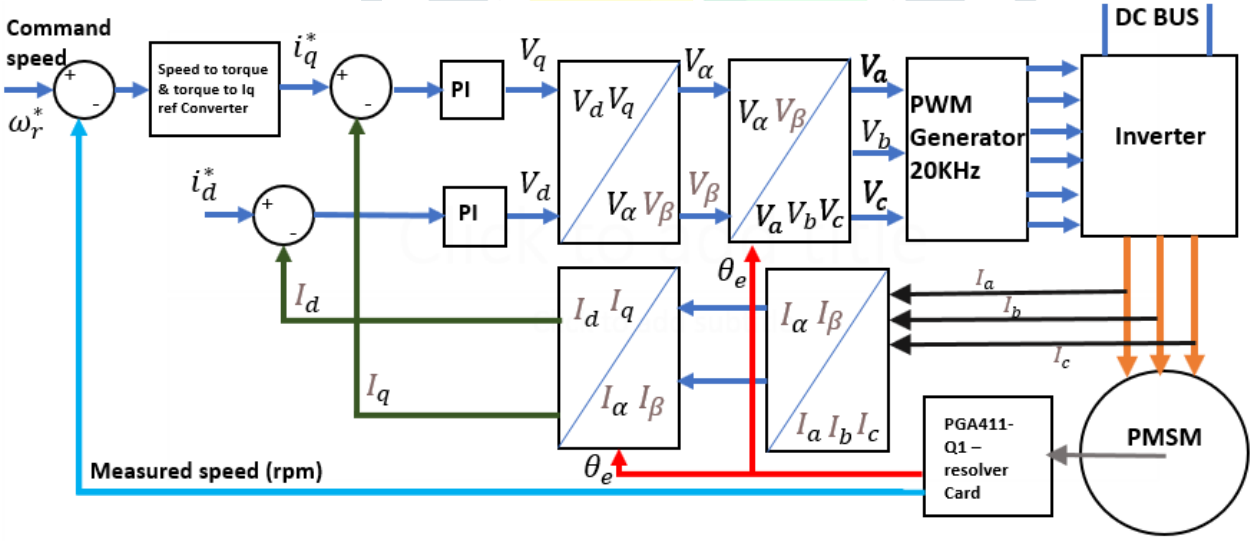

Fig 2. Functional Block Diagram of FOC algorithm

The position data of the rotor shaft of DUT motor is encoded using a position encoder. The position of the rotor shaft is decoded as the equivalent angular displacement (θ_r). The three phase currents I_a, I_b and I_c are considered as feedback inputs along with the position data. The three-phase time varying current components are transformed into equivalent two-phase time varying currents I_α and I_β in forward Clarke's transform using equations 3.1 and 3.2.

$$I_\alpha = \frac{2}{3}(Ia) - \frac{1}{3}(I_b + \bar{1}_c) \quad \text{.....(3.1)}$$

$$I_\beta = \frac{1}{\sqrt{3}}(I_b - I_c) \quad \text{.....(3.2)}$$

The two-phase equivalent time varying current components are transformed into two-time invariant orthogonal vectors I_d and I_q in forward Park's transform using equations 3.3 and 3.4.

$$I_d = I_\alpha \cos(\theta_r) + I_\beta \sin(\theta_r) \quad (3.3)$$

$$I_q = I_\beta \cos(\theta_r) - I_\alpha \sin(\theta_r) \quad (3.4)$$

The I_d and I_q currents signify the direct axis and quadrature axis current components of the permanent magnet motors. The direct axis component provides control of the air gap flux and the quadrature axis component provides the torque control of DUT motor. The DUT motor can be operated in torque mode by modulating the I_q component by varying I_q reference value. The DUT motor can be operated beyond the rated speed by modulating the I_d component by I_d reference value in flux weakening control.

The modulation of I_d and I_q components is done in PI controllers to obtain the voltage equivalent d-q components – V_d and V_q. The time invariant V_d and V_q vectors are transformed into two phase time varying voltage components V_α and V_β in inverse Park's transform using equations 3.5 and 3.6.

$$V_\alpha = V_q \cos(\theta_r) - V_d \sin(\theta_r) \quad (3.5)$$

$$V_\beta = V_d \sin(\theta_r) + V_q \sin(\theta_r) \quad (3.6)$$

The two-phase time varying voltage components are transformed to equivalent three-phase time varying components Va, V_b and V_c in inverse Clarke's transform using equations 3.7, 3.8 and 3.9.

$$V_a = V_\alpha \quad (3.7)$$

$$V_b = -\frac{1}{2}(V_\alpha) + \frac{\sqrt{3}}{2}(V_\beta) \quad (3.8)$$

$$V_C = -\frac{1}{2}(V_\alpha) - \frac{\sqrt{3}}{2}(V_\beta) \quad (3.9)$$

The three – phase voltages Va, V_b and V_c are compared with the high frequency triangle waves to generate the sinusoidal pulse width modulation (SPWM) signals in 180° conduction mode. The motor is operated through the inverter module using the generated SPWM signals.

3.2 METHODOLOGY

Fig.3 shows the flow diagram of the proposed methodology of the FOC algorithm with various modules in LabVIEW.

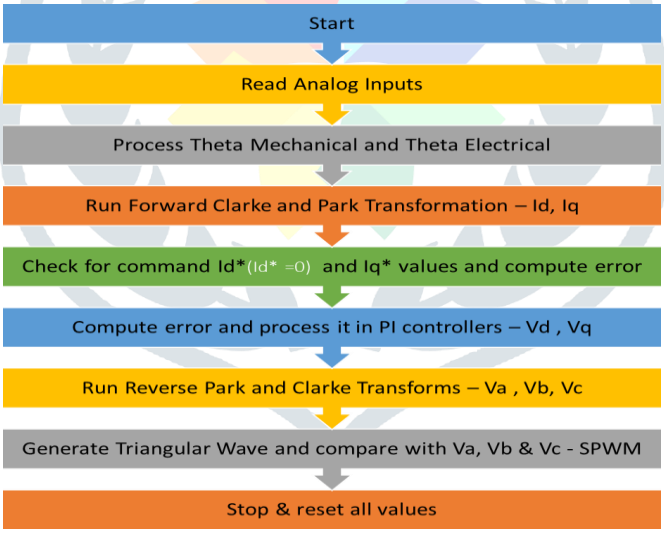

Fig 3. Flow chart of the proposed methodology

The proposed technique requires the per phase current and the actual rotor position and speed data to generate the control signals using the FOC algorithm in LabVIEW.

In Module – 1 (read analog inputs), the position of the rotor is obtained using the resolver mounted to the DUT motor shaft. The resolver data is obtained as continuous sine and cosine signals. These continuous sine and cosine signals are processed as an up-ramp voltage varying from 0.4V to 4.5V in the resolver decoder. The phase currents are also obtained as variable voltage signals through current sensors as feedback input to the FOC algorithm. The analog data is passed to FPGA NI 9223. The position signals are normalized to obtain the mechanical angular displacement values. (θ_m).

In Module - 2 (Theta M to Theta E), the theta mechanical values are then normalized to vary from 0 to 2π radians using the equation 3.10. The equivalent electrical angular displacement (θ_e) is obtained by the conversion of theta mechanical to theta electrical using the equation 3.11.

$$\theta_m = \frac{ResVoltage - V_{min}}{V_{max} - V_{min}} \times 2\pi \text{ [rad]} \quad (3.10)$$

$$\theta_e = \frac{P}{2}\theta_m \text{ [rad]} \quad (3.11).$$

Module-3 (Forward Clarke's Transform) The three phase currents I_a, I_b and I_c aretransformed in to two phase equivalent orthogonal currents I_α and I_β. The three - phase stationary reference phasors are transformed to equivalent two phase orthogonal stationary reference currents in forward Clarke transform.

In module-4 (Forward Park's Transform), The two-phase orthogonal stationary reference equivalent currents I_α and I_β are transformed into two phase equivalent orthogonal rotating reference current vectors I_d and I_q. I_d is the direct axis component which is considered at rotor pole's maximum flux interaction with stator poles, the I_d component is also considered as flux controlling component. I_q is in quadrature to I_d at the quadrature axis, the I_q component is considered as the torque controlling component.

In module 5 (PI Controllers), On performing the Clarke and Park transforms, the AC quantities are now considered in Synchronous rotating reference frame eliminating the frequency, thus the I_d and I_q values are equivalent DC components of three phase AC components. The Command Speed reference value is fed to the controller. The error in speed is converted to equivalent torque current command Iq*. The equivalent command torque current 'Iq*' and flux current 'Id*' (Id =0) are computed and fed to the PI controllers.

In module-6 (Inverse Park's Transform), The inverse Park transformation (dq0 to alpha beta 0) transforms the signals (V_q and V_d voltages) in the rotating reference frame to two phase stationary reference frame. The two orthogonal DC components are now considered as two-phase orthogonal AC equivalent components V_α and V_β.

In Module-7 (Inverse Clarke's Transform), The two-phase AC voltages are converted to the three phase voltages V_a, V_b and V_c.

In Module 8, (SPWM Generator), The triangular wave is generated at high frequencies equivalent to the switching frequency of 5kHz. The 3 phase Sine waves V_a, V_b and V_c obtained is normalized and then is sampled using the high frequency triangular wave to generatethe SPWM pulses.

IV. SPECIFICATIONS AND DESIGN DETAILS

The hardware systems considered in the implementation of the FOC algorithm in LabVIEW is as follows.

1. **Selection of Motor**

The motor considered is an 8-pole interior permanent magnet, IPM - PMSM motor with 41 KW – continuous power and 60KW peak power. The base speed of the motor is 2800 rpm and the peak speed is 5000 rpm. The voltage rating of the DUT motor is 150 V, with peak current rating of 450 A.

2. **Selection of Resolver**

The Resolver is also the 8-pole hollow shaft resolver – 2367254-1 is used to match the motor pole pairs.

3. **Selection of Inverter**

The inverter is chosen based on the maximum switching frequency required to operate the motor at the top most speed. The maximum Switching frequency considered is 12 kHz and the minimum optimal switching frequency is 2kHz. The Semikron Inverter SKAI 45 A2 GD12-WDI is considered The DC input voltage = 800V, DC input current = 300A, 12kHz switching frequency IGBT module.

4. **Resolver Decoder**

The resolver's sine and cosine signals are converted to the real time analog voltage signals observed as an up-ramp signal varying from 0.4V to 4.5 V, using Texas Instruments PGA411-Q1 development board.

5. **Selection of Real time interface**

The National Instruments CRIO9046, NI9401 and NI9223 modules are used for real time interface, where CRIO9046 is an FPGA interface cubicle and NI9223 is the high-speed analog input (AI- 1MS/s) FPGA module and NI9401 is the high-speed digital input – output (DIO- 10MHz) FPGA module.

V. SIMULATION ANALYSIS AND DISCUSSION

5.1 MATLAB model of the FOC algorithm

The vector control algorithm – FOC for the direct torque control and the flux weakening control of the DUT motor in torque mode is designed using the mathematical model of PMSM motor and the simulation results are verified with mathematical values obtained.

The Mathematical model of the motor is considered based on the desired torque and speed values to be achieved by the motor using the following equations.

$$\frac{di_d}{dt} = \frac{1}{L_s}\left[V_d - Ri_d + \omega L_s i_q\right] \quad (5.1)$$

$$\frac{di_q}{dt} = \frac{1}{L_s}\left[V_q - Ri_q - \omega L_s i_d - \omega\psi\right] \quad (5.2)$$

$$T_e = 1.5P\left[\lambda i_q + \left(L_d - L_q\right)I_d I_q\right] \quad (5.3)$$

$$\frac{d\omega}{dt} = \frac{1}{J}T_e \quad (5.4)$$

The inductance, resistance of the windings of the motor, air gap flux, torque and inertia of the motor are known from the equations. The mathematical model of the PMSM motor is developed as shown in fig 4.

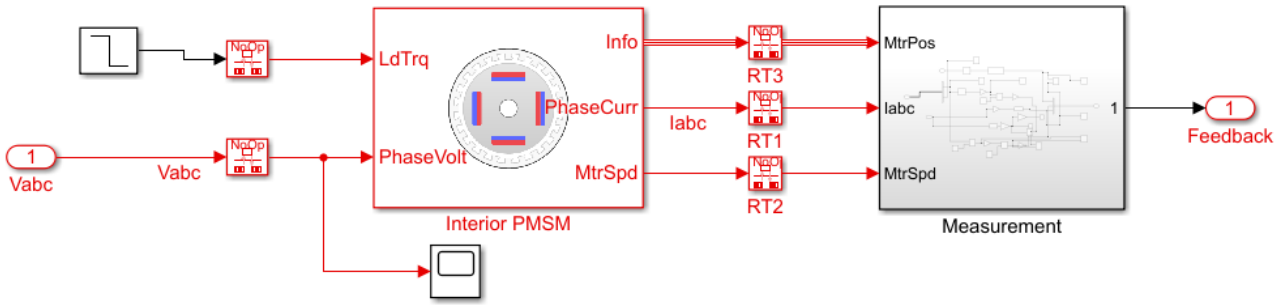

Fig.4 MATLAB model of PMSM DUT motor

The Interior PMSM motor is simulated with a constant light load torque of 8E-3 Nm. The Motor's rotor position and speed is sensed using the resolver to get Theta Mechanical – angular displacement. The Currents from each phase is taken as feedback from motor terminals – Ia, Ib and Ic.

5.2 Mechanical angular displacement to Electrical angular displacement

The rotor position is identified as ramp signals which is obtained by the resolver decoder. The measured rotor position is normalized to vary from 0 to 2π radians using equation 3.10. Each mechanical rotation is considered as one mechanical angular displacement (θ_m) and the equivalent electrical angular displacement (θ_e) using equation 3.11. The electrical equivalent rotation of the mechanical rotation, depends on the number of poles of the motor.

The Block Diagram of Resolver data and computation of θ_m and θ_e values simulated in MATLAB is shown in fig 5.

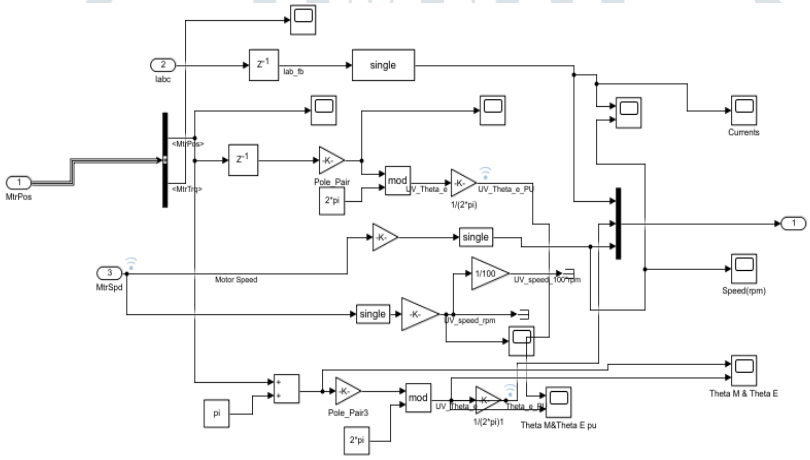

Fig.5. Computing θ_m and θ_e in MATLAB

Fig 6 shows the θ_m and θ_e values plotted in MATLAB

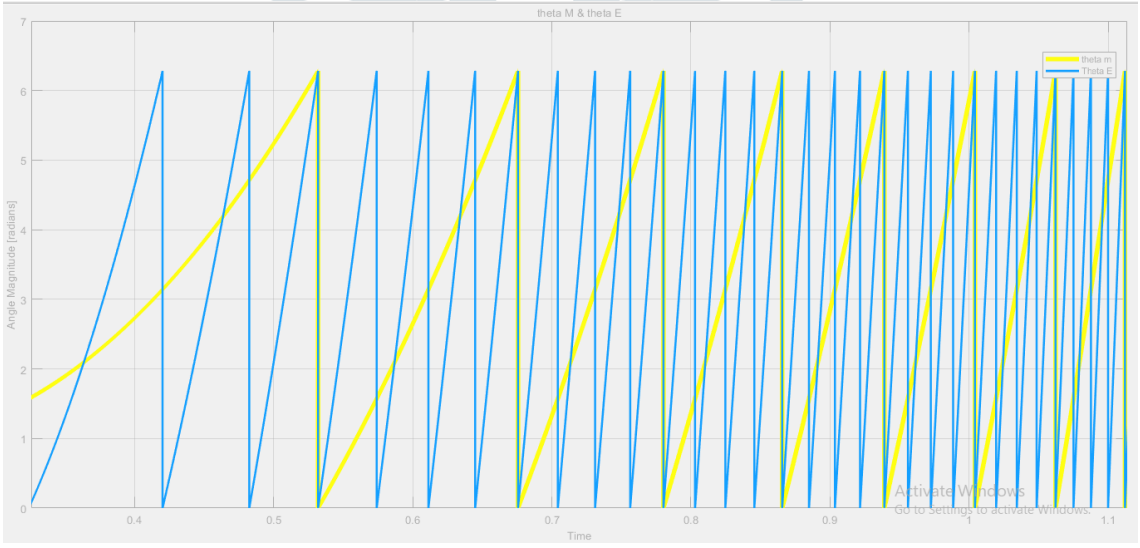

Fig.6. Plotting θ_m and θ_e in MATLAB

The Currents from each phase is considered as the feedback for the forward Clarke's and Park's transformations is shown in fig 7.

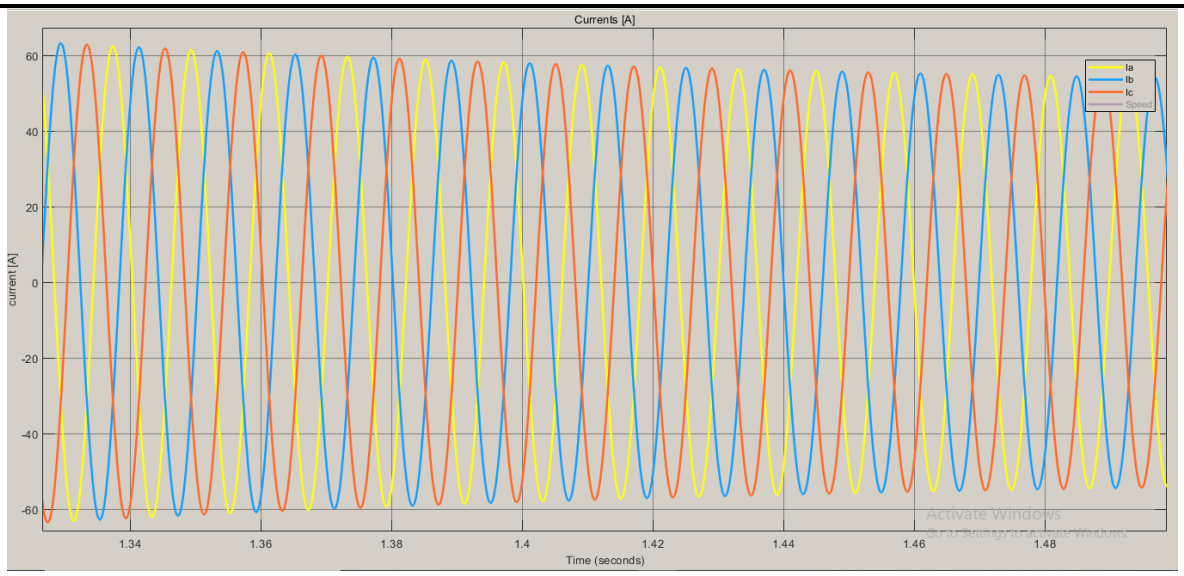

Fig 7. Currents from each phase – I_a, I_b and I_c

The control blocks of the FOC – forward Clarke's transform, forward Park's transform and reverse Park's transform and reverse Clarke's transformations is shown in fig 8.

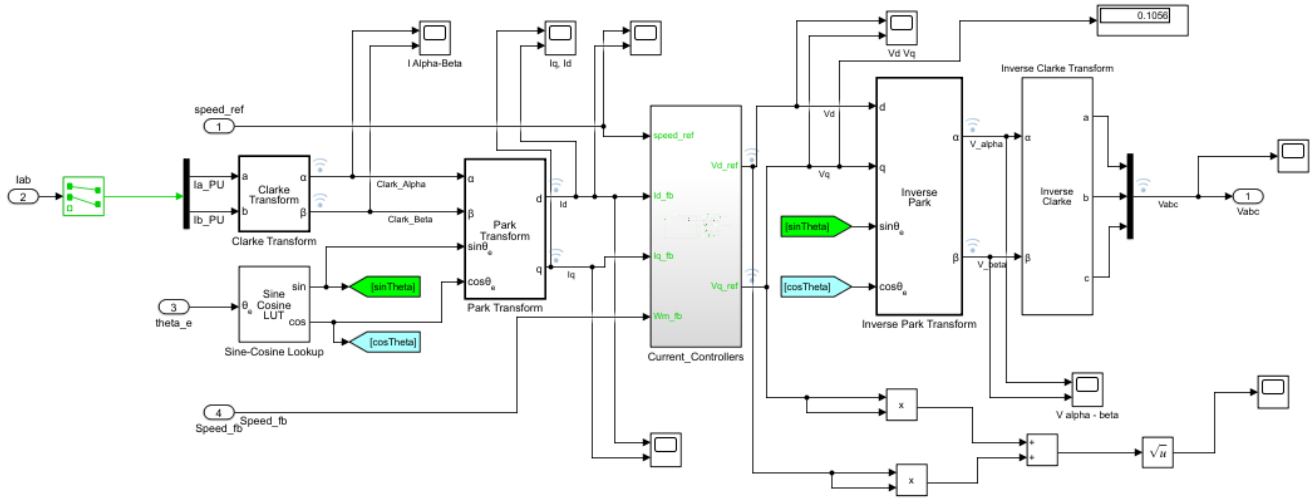

Fig 8 FOC Blocks – forward Clarke's, forward Park's transform and reverse Park's, reverse Clarke's transformations

5.3 Forward Clarke's Transform

The three phase currents I_a, I_b and I_c aretransformed in to two phase equivalent orthogonal currents I_α and I_β. The three - phase stationary reference phasors are transformed to equivalent two phase orthogonal stationary reference currents in forward Clarke transform using equations 3.1 and 3.2. The orthogonal currents I_α and I_β are plotted in MATLAB, shown in fig 9.

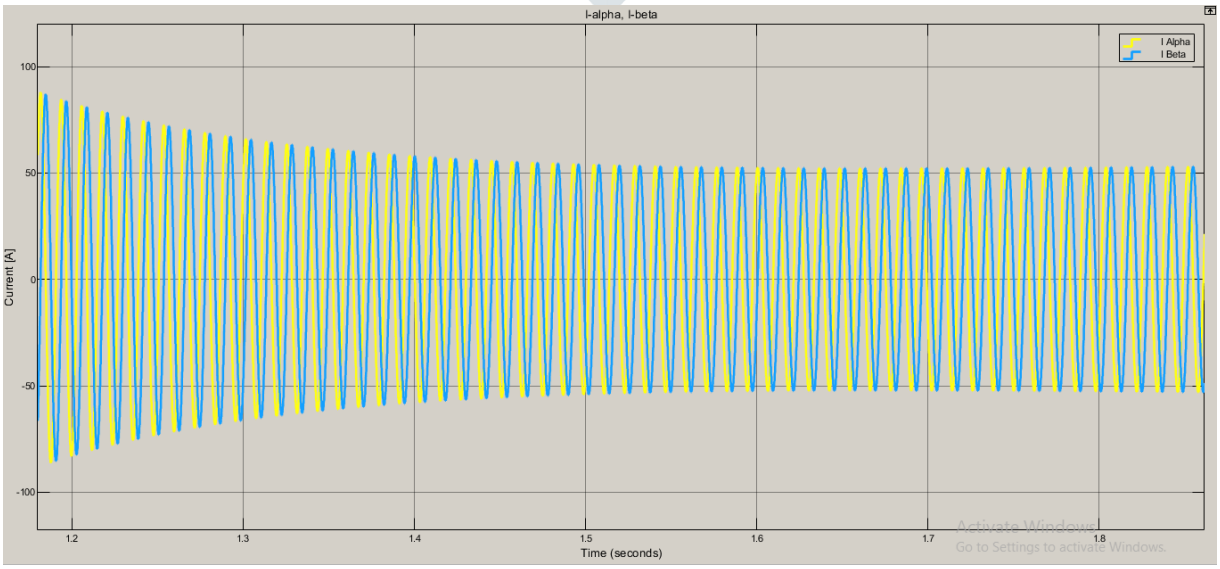

Fig.9 Currents I_α and I_β plotted in MATLAB

5.4 Forward Park Transform

The two-phase orthogonal stationary reference equivalent currents I_α and I_β are transformed into two phase equivalent orthogonal rotating reference current vectors I_d and I_q, using equations 3.3 and 3.4. The two-phase equivalent orthogonal current vectors I_d and I_q is shown in fig.10.

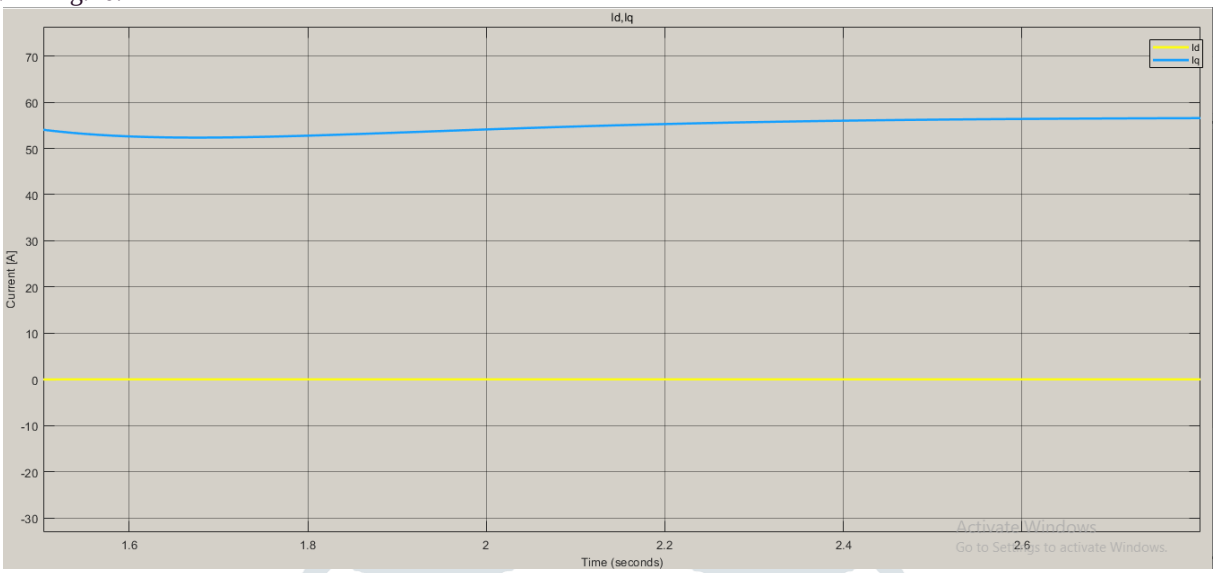

Fig.10 Orthogonal rotating reference current vectors I_d and I_q

5.5 PI Controllers Block

On performing the Clarke and Park transforms, the time varying AC quantities are now considered in Synchronous rotating reference frame eliminating the frequency, thus the I_d and I_q values are equivalent DC components of three phase AC components. The Command Speed reference value is set to the controller. The error in speed is converted to equivalent torque current command Iq*. The equivalent command torque current 'Iq*' and flux current 'Id*' (Id =0) are computed and fed to the PI controllers to obtain the correction modulated voltage d-q components V_d and V_q. The proportional gain - Kp and integral gain - K_i, values for parallel PI controller is computed for the DUT PMSM motors using the following equations 5.1 and 5.2.

$$K_P = L_s\omega_0 \quad \text{.....(5.1)}$$

$$K_i = R\omega_0 \quad \text{.....(5.2)}$$

Where: L_s is the Line inductance between RY phases
R is the Line resistance between RY phases
ω_0 is the current bandwidth

The correction modulated output d-q voltage components, Vd and Vq are plotted in MATLAB as shown in Fig.11.

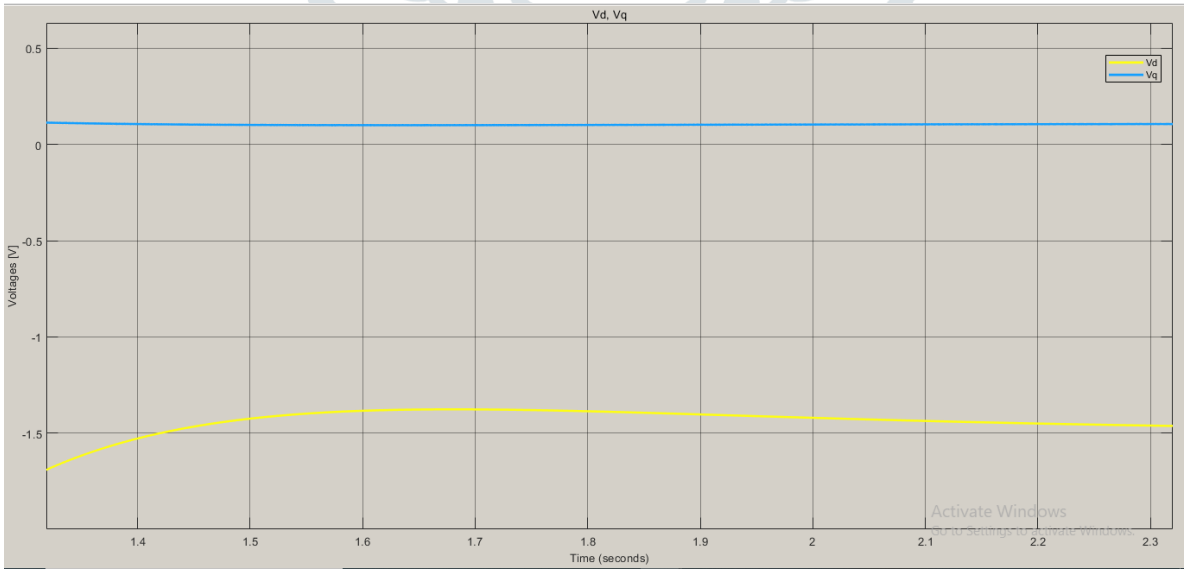

Fig.11 Vd and Vq are plotted in MATLAB

5.6 Inverse Park Transform

The inverse Park transformation (dq0 to alpha beta 0) transforms the signals (V_q and V_d voltages) in the rotating reference frame to two phase stationary reference frame. The two orthogonal DC components are now considered as two-phase orthogonal AC equivalent components V_α and V_β using equations 3.5 and 3.6. Fig.12 shows the plot of V_α and V_β.

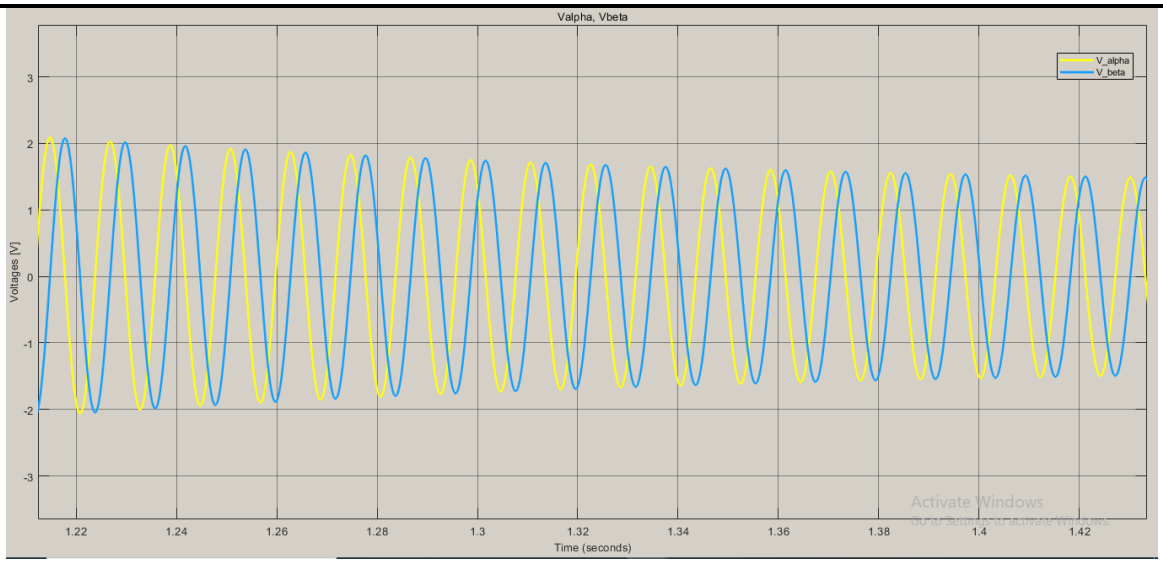

Fig.12 V_α and V_β plotted in MATLAB

5.7 Inverse Clarke's transform

The two-phase AC voltages are converted to the equivalent three phase voltages V_a, V_b and V_c using equations 3.7,3.8 and 3.9. The three phase voltages V_a, V_b and V_c are plotted in MATLAB, shown in Fig.13.

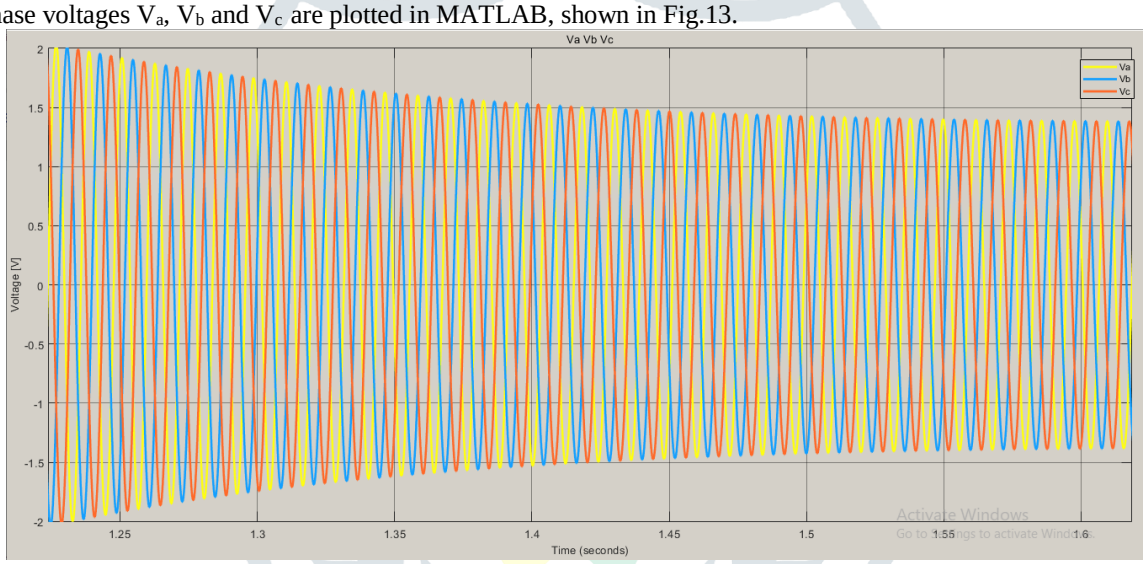

Fig.13 three phase voltages V_a, V_b and V_c are plotted in MATLAB

5.8 Sinusoidal Pulse Width Modulation (SPWM)

The three – phase voltages Va, V_b and V_c are compared with the high frequency triangle waves to generate the sinusoidal pulse width modulation (SPWM) signals in 180º conduction mode. The motor is operated through the inverter module using the generated SPWM signals. The block diagram of SPWM logic simulated in MATLAB is shown in Fig.14.

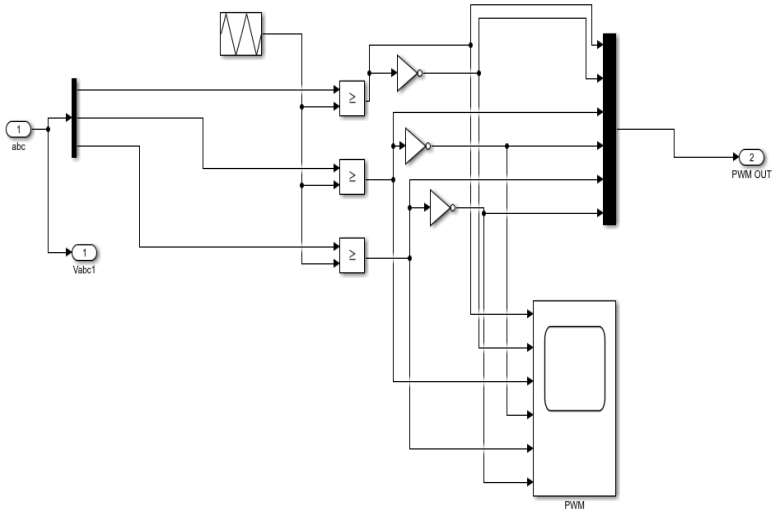

Fig.14 SPWM logic for 180º conduction mode

The sinusoidal PWM signals generated in MATLAB is as shown in fig.15.

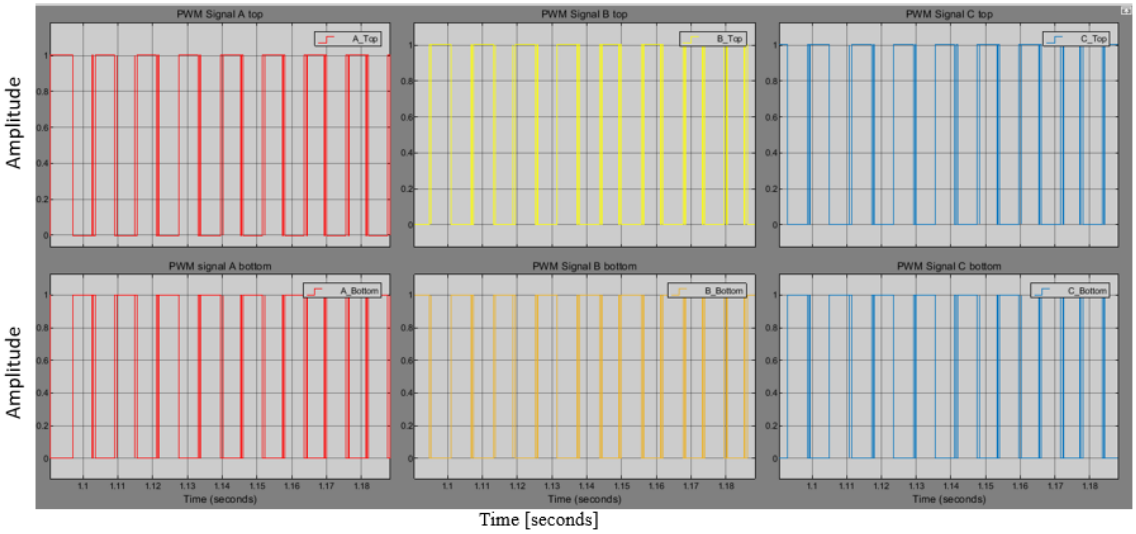

Fig.15 Sinusoidal PWM signals generated in MATLAB

The speed and torque response of the FOC algorithm simulated in MATLAB for set speed of 5000 rpm with load torque of 80mNm is shown in Fig.16 and Fig17.

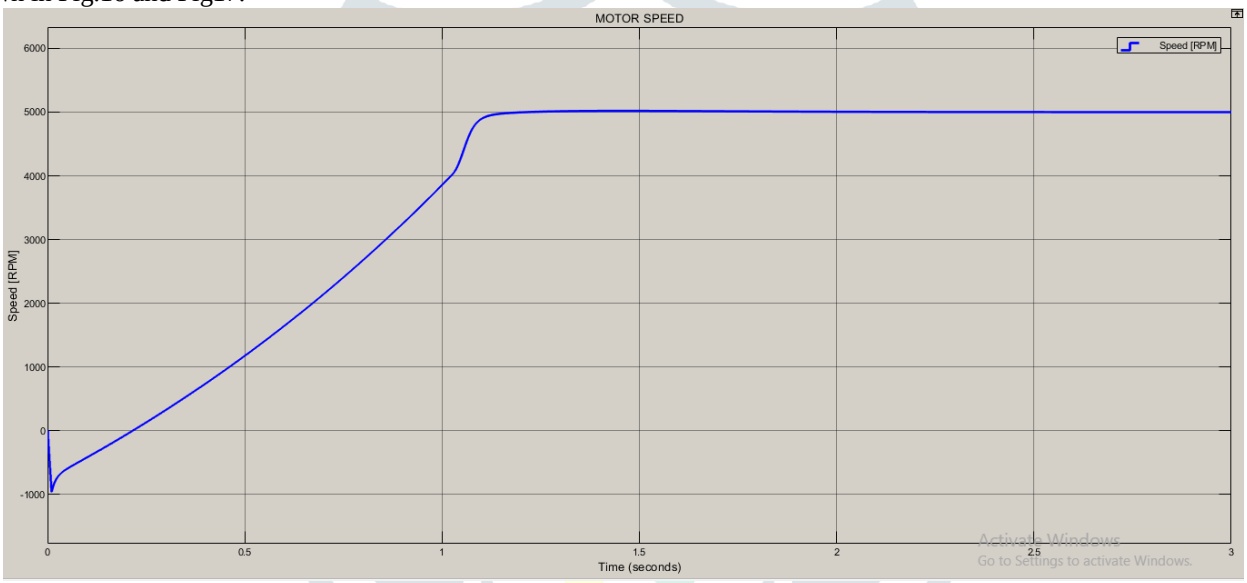

Fig.16 Motor Speed response in MATLAB at 5000 rpm.

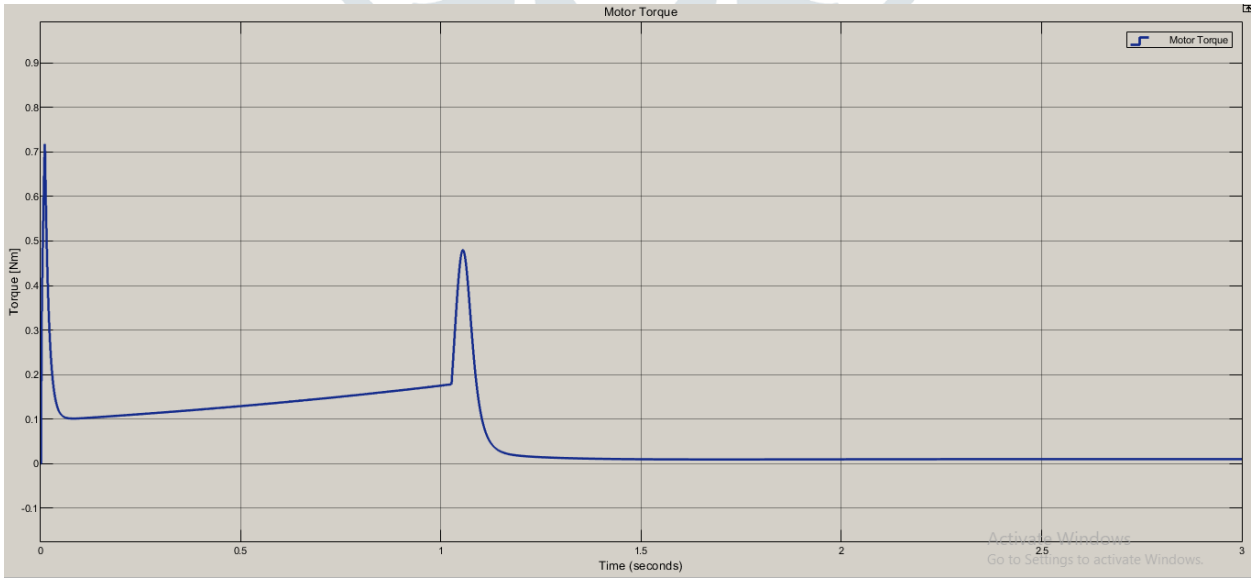

Fig.17 Motor Torque response in MATLAB at 80mNm.

VI. HARDWARE IMPLEMENTATION RESULTS AND DISCUSSION

6.1 Graphical User Interface

The graphical user interface (GUI) designed for speed setting and monitoring real time data is shown in Fig.18.

Fig.18 GUI developed for FOC in LabVIEW

6.2 Hardware Results of FOC Control of DUT Motor

The DUT- PMSM motor is tested in 350kW dyne test bench to operate in forward motoring, forward braking, reverse motoring, and reverse breaking operations by applying varying loads on the DUT motor by dyne motor.

1. **Forward Motoring**
   - The Motor is loaded on 350kW Dyne system with 120V DC supplied to inverter.
   - The Motor is operated in forward direction.

Table-1 shows the variation of speed for load conditions of DUT motor

Set Speed [rpm]	Iq ref [A]	R- Phase Current [A]	Actual Speed [rpm]	Load [Nm]
800	50	40-50	830	10
2000	60	50-60	2050	12
2000	70	60-70	1900	14
2000	75	60-75	1890	18
2000	80	70-80	1850	22

Table-1 Variation of speed for varying load in forward direction

2. **Reverse Motoring**
   - The Motor is loaded on 350kW Dyne system with 120V DC supplied to inverter.
   - The Motor is operated in reverse direction.
   - The negative sign indicates that the rotor shaft direction is in opposite direction from previous case.

Table-2 shows the variation of speed for load conditions of DUT motor in reverse direction

Set Speed [rpm]	Iq ref [A]	R- Phase Current [A]	Actual Speed [rpm]	Load [Nm]
-800	50	40-50	-800	10
-2000	60	50-60	-1950	12
-2000	70	60-70	-1900	14
-2000	75	60-75	-1890	18
-2000	80	70-80	-1850	22

Table-2 Variation of speed for varying load in reverse direction

6.3 Hardware Results – Sinusoidal PWM signals

The 180-degree conduction mode- sinusoidal PWM signals from the developed FOC algorithm is read at the FPGA module NI-9401 ultra-high speed DIO pins – 0 to 5. The sinusoidal PWM signals are then amplified from 5V to 12V.The PWM signals generated are shown in Fig.19.

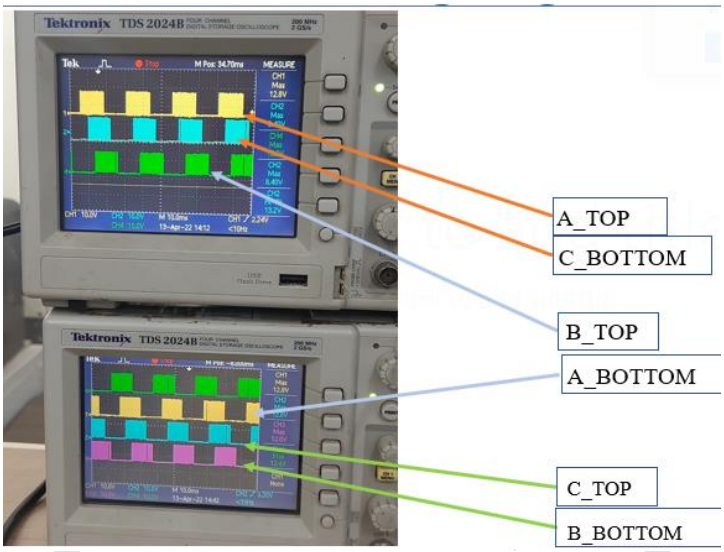

Fig.19 Sinusoidal PWM signals generated in 180-degree conduction mode

6.5 Hardware Results – Line Voltages across the DUT motor terminals

The line Voltages across RY, YB and BR phases on no-load condition are as shown in Fig.20.

Fig.20 Line Voltages across RY, YB and BR terminals of the DUT motor on no-load

Table-3 shows the measured values of the line voltages of DUT motor in no load conditions.

Phase	V_{max}[V]	V_{min} [V]	V_{rms} [V]	V_{pk-pk} [V]
R-Y	49.6	-51.2	25.3	101
Y-B	52.2	-49.5	25.4	102
B-R	49.5	-52.0	25.2	101

Table -3 Measured Line voltages of DUT motor on no-load

6.6 Hardware Results – Phase Voltages across the DUT motor terminals

The phase voltages across each phase terminals with respect to dedicated neutral wire of the DUT motor is shown in Fig 21.

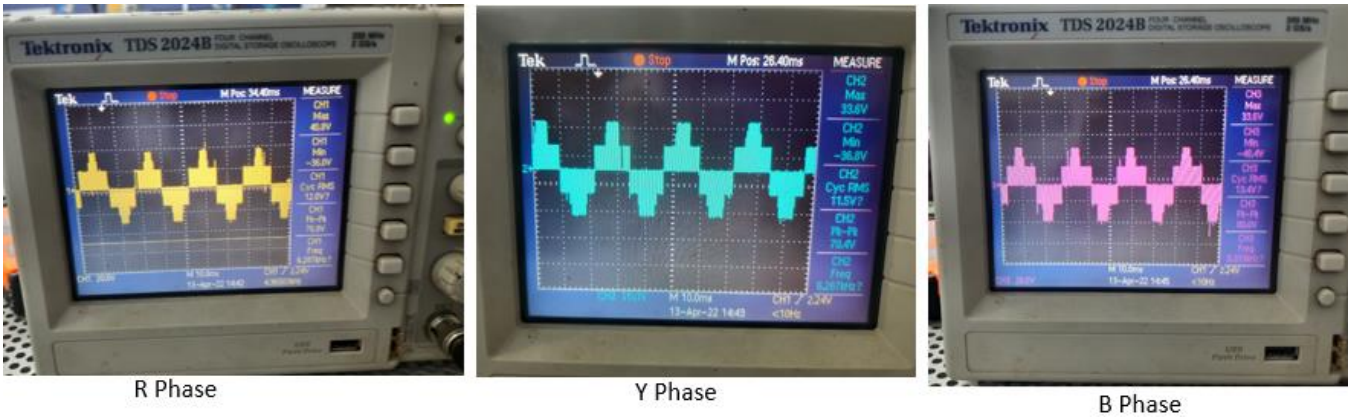

Fig.21 Phase voltages across each phase terminals with respect to dedicated neutral wire of the DUT motor

Table-4 shows the measured phase voltages across each phase and dedicated neutral wire of the DUT motor

Phase	V_{max}[V]	V_{min} [V]	V_{rms} [V]	V_{pk-pk} [V]	Frequency [kHz]
R	33.3	-36	12	70	6.26
Y	33.6	-36.8	11.5	70.4	6.28
B	33.6	-36.4	13.4	70	6.3

Table-4 Phase voltages across each phase terminals with respect to dedicated neutral wire of the DUT motor

VII. CONCLUSION

The developed program in LabVIEW software offers robust control of the DUT - PMSM motor in torque mode. The DUT motor reaches the set speed on no-load condition in 3 seconds and on-load condition at 10Nm, the motor reaches the set speed of 800rpm in 6 seconds. The DUT motor drives the load at set speed with variation in phase currents compared with the set reference current of corresponding speed. The error in set reference current and measured current is observed to be less than +/-10%. The developed module operates the DUT motor in all 4 quadrant operations and performance analysis is conducted on Dyne test bench.

REFERENCES

[1] Gora, R., Biswas, R., Garg, R.K. and Nangia U, "**Field Oriented Control of Permanent Magnet Synchronous Motor (PMSM) Driven Electric Vehicle And Its Performance Analysis**". *In 2021 IEEE 4th International Conference on Computing, Power and Communication Technologies (GUCON)* September 2021,pp. 1-6.

[2] O. Tahmaz, M. N. Ekim and A. B. Yildiz, "**Vector Control of Permanent Magnet Synchronous Motor by a Two-Level SPWM Inverter**," *2020 4th International Symposium on Multidisciplinary Studies and Innovative Technologies (ISMSIT)*, 2020, pp. 1-7.

[3] Tatar G, Korkmaz H, SERTELLER NF, TOKER K, " LabVIEW FPGA based BLDC Motor Control by using field oriented control algorithm". *In 2020 IEEE International Conference on Smart Energy Systems and Technologies* (SEST) 7 Septempber 2020 PP. 1-6.

[4] Wang, Z., Chen, J., Cheng, M. and Chau, K.T., "**Field-oriented control and direct torque control for paralleled VSIs fed PMSM drives with variable switching frequencies**". *IEEE Transactions on Power Electronics*, *31*(3),March 2016, pp.2417-2428.

[5] P. Kumar, S. Dhundhara and R. Makin, **"Performance analysis of PMSM drive based on FOC technique with and without MRAS method,"** *2016 International Conference on Recent Advances and Innovations in Engineering (ICRAIE), 16 May* 2016, pp. 1-6.

[6] Liu, Y., Barford, L. and Bhattacharyya, S.S, **"Constant-rate clock recovery and jitter measurement on deep memory waveforms using dataflow".** In *2015 IEEE International Instrumentation and Measurement Technology Conference (I2MTC) Proceedings*,2015, May PP. 1590-1595.

[7] X. Zhai, M. Zhang, X. Bai and Z. Zhang, **"A Signal Analysis Design Based on LabVIEW,"** *2015 International Conference on Cyber-Enabled Distributed Computing and Knowledge Discovery*, 2015, PP. 473-476.

[8] Bevilaqua MA, Nied A, de Oliveira J, **"Labview fpga foc implementation for synchronous permanent magnet motor speed control"**. *In 2014 11th IEEE/IAS International Conference on Industry Applications* 2014 Dec 7 PP. 1-8.

[9] F. Yusivar, N. Hidayat, R. Gunawan and A. Halim, **"Implementation of field oriented control for permanent magnet synchronous motor,"** *2014 International Conference on Electrical Engineering and Computer Science (ICEECS)*, 2014, PP. 359-362.

[10] E. Yesilbag and L. T. Ergene, **"Field oriented control of permanent magnet synchronous motors used in washers,"** 2014 16th International Power Electronics and Motion Control Conference and Exposition, 2014, PP. 1259-1264.

[11] Feng, C., Jia-Xiong, Z. and Ji-Hao, Y., **"Frequency spectrum analysis of sampling clock jitter system based on LabVIEW "**, In *2012 International Conference on Computational Problem-Solving (ICCP)* 2012, October, PP. 325-327.

[12] J. Kryszyn, D. Wanta, P. Kulpanowski and W. T. Smolik, "**LabVIEW based data acquisition system for electrical capacitance tomography**," 2018 International Interdisciplinary PhD Workshop (IIPhDW), 2018, pp. 348-352.

[13] H. M. Wang, D. D. Li, P. Xue, J. Zhu and H. B. Li, "**LabVIEW-based data acquisition system design**," Proceedings of 2012 International Conference on Measurement, Information and Control, 2012, pp. 689-692.

[14] Y. Luo, C. G. Li, F. Zhang and K. Wang, "**The real-time monitor system based on LabVIEW**," Proceedings of 2012 International Conference on Computer Science and Network Technology, 2012, pp. 848-851.

[15] Mirahki, H. and Moallem, M. "**Torque calculation in interior permanent magnet synchronous machine using improved lumped parameter models**". *Progress in Electromagnetics Research M*, *39*, 2004 pp.131-139